Detection of Incipient Object Slippage by Skin-Like Sensing and Neural Network Processing

Gaetano Canepa, Rocco Petrigliano, Matteo Campanella, and Danilo De Rossi

Abstract—**Detection of incipient slippage is of great importance in robotics for the control of grasping and manipulation tasks. Together with fine-form reconstruction and primitive recognition, it has to be the main feature of an artificial tactile system. The system presented here is based on a neural network used to detect incipient slippage and on a skin-like sensor sensible to normal and shear stresses. Normal and shear stresses components inside the sensor are the input data of the neural net. An important feature of the system is that the *a priori* knowledge of the friction coefficient between the sensor and the object being manipulated is not needed. To validate the method we worked on both simulated and experimental data. In the first case, the Finite Element Method is used to solve the direct problem of elastic contact in its full nonlinearity by resorting to the lowest number of approximations regarding the real problem. Simulation has shown that the network learns and is robust to noise. Then an experimental test was carried out. Experimental results show that, in a simple case, the method is able to detect the incipiency of slippage between an object and the sensor.**

I. Introduction

UNTIL now, two principal methods have been presented to obtain optimal grasp force avoiding (or controlling) the slippage of the manipulated object. The first method was presented by Bicchi *et al.* [1], [2]: in this case the robot performs, through exploration, an estimation of the friction coefficient (μ) between a force-torque tactile sensor and the manipulated object. Using this estimated value of μ it is possible, by measuring the normal and tangential components of the contact force, to avoid slippage during manipulation. Problems arise in the case of occurrence of twisting moments [3]; in such a case, the slip condition depends on the distribution of normal and tangential stress in the contact area.

A second method has been proposed by Cutkosky *et al.* [4], [5]. They detect incipient slippage by sensing microvibrations caused by the propagation of the slip regions within the contact area as the tangential force increases (see Section II). Vibrations are detected using a couple of accelerometers: an accelerometer, placed near the contact area, is particularly sensitive to vibrations caused by slip-zone widening, while the second, far from the contact zone, is used to limit the influence of environmental noise. Studies in neuro-physiology [6] demonstrate that human beings perceive sliding in correspondence with firing activity of Pacini corpuscles (the tactile receptors sensitive to high frequency vibrations). Monitoring vibrations to detect incipient slippage seems, for this reason, to be natural. This method has the advantage of working without the knowledge of μ (on the contrary this method can give a measure of μ as a result of a manipulative act) and it does not use sophisticated sensor arrays, but just two simple accelerometers. On the other side, this method is vulnerable to numerous artifacts due to environmental vibrations and to vibrations generated during multifinger manipulation (joint vibration and cross-sensor noise).

Other methods have been proposed [7] but they do not appear to be particularly useful, since they essentially measure slippage when it already occurred.

Two studies are presented here, related to the use of a tactile sensor array to detect incipient slippage. We designed and realized a tactile sensor selectively sensitive to shear and normal stress components generated during frictional contact. In the first part of the study we present here, we worked only on simulated data. They were obtained through the finite element technique and they were used to produce the input signal necessary for validating the method and to select the best network structure. The preliminary results of this study [8] were encouraging but they need experimental verification: the second part of the study was carried out for this purpose.

A neural net, whose inputs are the shear and normal stresses sampled at the transducer level (both simulated and experimental), provides as output a global *sliding coefficient*. This coefficient is ideally equal to the ratio $\frac{Q}{\mu P}$, where Q and P are, respectively, the tangential and the normal reaction on the surface of the sensor. Consequently, when the output of the network is near to 1, the contact is near to the sliding condition. The advantages of the use of this technique are:

- high immunity to vibration noise;
- possibility of an easy integration with already developed neural networks for *fine-form reconstruction* [9], [10];
- high speed and suitability for closed-loop control of grasping and manipulation.

Experimental data are obtained using a simple prototype of an array tactile sensor we developed. The sensor is described in Section III.

This paper is structured as follows. First, the incipient slippage condition is described in terms of contact mechanics, and the sensor design is briefly outlined; then we report a description of the approach used to find the solution of the direct problem by means of the Finite Element Method (FEM) to obtain simulated data; subsequently the structure of the neural network used to achieve the solution of the

Manuscript received November 7, 1995; revised March 2, 1997. This work was supported in part by Du Pont de Nemours Italiana S.p.A.

The authors are with Centro "E. Piaggio," Facoltà di Ingegneria, Università di Pisa, 56126 Pisa, Italy (e-mail: gaetano@pimac2.iet.unipi.it).

Publisher Item Identifier S 1083-4419(98)03514-6.

inverse problem, for both simulated and experimental data, is discussed; finally, experimental results are reported.

II. Incipient Slippage Condition

From contact mechanics [11], it is known that a tangential force whose magnitude is less than the force of limiting friction, when applied to two bodies pressed into contact, will not cause a sliding motion but, nevertheless, will induce frictional traction at the contact interface. It can be shown that a small relative motion (referred to as "microslip") over part of the interface occurs also when the tangential force is inferior to the limiting friction force ($Q < \mu P$). The remainder of the interface deforms without relative motion and in such regions the surfaces are said to adhere or to "stick." As it has been said in the introduction, the slip area propagation produces micro-vibrations (particularly in proximity of incipient slippage condition). At the points within the stick region the local shear traction does not exceed its limiting value. Assuming Amonton's law of friction with a constant coefficient μ, this restriction may be stated

$$|q(x,y)| \leq \mu |p(x,y)| \tag{1}$$

where $q(x,y)$ and $p(x,y)$ are tangential and normal traction fields, respectively. Moreover, points located in a "stick" region must have a null slip.

Indicating rigid displacements at the points that are far from the contact region with δ_x and δ_y and elastic displacements at the stick contact region by $\bar{u}_x$ and $\bar{u}_y$. the following equations must be satisfied:

$$\begin{aligned} \bar{u}_{x1} - \bar{u}_{x2} &= (\delta_{x1} - \delta_{x2}) \equiv \delta_x \\ \bar{u}_{y1} - \bar{u}_{y2} &= (\delta_{y1} - \delta_{y2}) \equiv \delta_y \end{aligned} \tag{2}$$

where indexes 1 and 2 indicate two (normal and tangential) load situations without complete slippage. In a slip region, the tangential and normal traction are related by

$$|q(x,y)| = \mu |p(x,y)|. \tag{3}$$

In addition, the direction of the frictional traction q must be the opposite of slip direction. Thus

$$\frac{q(x,y)}{|q(x,y)|} = -\frac{s(x,y)}{|s(x,y)|} \tag{4}$$

where $s(x,y)$ represents the displacement along X axis, relative to the origin, of a generic point having coordinates (x,y). Equations (1)–(4) provide boundary conditions which must be satisfied by the surface tractions and surface displacements at the contact interface. Equations (1) and (2) apply to a stick region, and (3) and (4) apply to a slip region.

On these grounds, the ratio of the extensions of the stick and slip regions over the interface would appear to be a good index of the incipient slippage state, as well as the ratio $S_i = \frac{Q}{\mu P}$ [8].

In this work we wanted to teach to a neural network to detect the slippage index directly from the measurement of the stress field inside the sensor. To obtain this result we built a learning set composed of couples of normal and shear stress field measurements in the sensor. To each data is associated a certain value of S_i. The S_i value is obtained in two different ways.

- In the case of simulated contact, S_i is obtained by calculating the resultant of the tangential and normal reactions, and assuming the relation $\frac{Q}{\mu P} = 1$ valid in incipient slippage conditions.
- In the case of real data, S_i is given by measuring the friction limit angle ($\theta_L = \arctan(\mu)$) between the indenter and the sensor rubber layer (see Fig. 6); then

$$S_i = \frac{Q}{\mu P} = \frac{Q}{\tan(\theta_L) P} = \frac{\tan(\theta)}{\tan(\theta_L)} \tag{5}$$

where θ is the angle between the force applied to the indenter and the perpendicular to the sensor surface.

III. A Tactile Sensor for Incipient Slip Detection

Incipient slippage can be detected by the progressive shape changes of the stress spatial distributions inside the sensor block due to an incremental tangential load acting on the pressing body, while maintaining a constant normal load [8], [12].

To detect the incipience of slippage we developed a sensor that is able to measure two components of the internal stress field generated by the contact with different objects (see Fig. 1). It consists of a linear array of eight couples of piezoelectric polymer transducers: one transducer of each couple is sensitive to a combination of normal stresses [13], while the other detects the shear stress along the direction of the array. The real sensor cannot have higher spatial resolution because the transducer needs to have a big area to enhance the signal to noise characteristic.

Fig. 1 depicts the sensor. It is a multilayer structure made of a 1-cm thick Aluminum base used to fix the sensor to the test structure. On the aluminum base is fixed, by means of four screws, a custom printed circuit on which the metal contacts for the transducers are photolithographically engraved. Two different types of piezoelectric polymer films are then glued, with cyanoacrylic glue, on the printed circuit. A layer of conductive paint is distributed on the polymeric layer to realize the ground contact. Finally, a 1.5-mm thick layer of natural rubber completes the structure.

Some tricks are necessary to obtain a reasonably good signal from the sensor. In fact, the two polymeric films used in the sensor are obtained in two ways and present different behavior while force or temperature on the transducer change. A layer, the one sensitive to a combination of normal stresses, is made of a 28-μm thick two-axial PVDF film (from Solvay & Cie, Bruxelles, Belgium). The other layer is made of a 60-μm thick PVDF film obtained cutting with a microtome a 1-mm thick sheet of mono-axial PVDF (from Thomson CSF, Paris, France), perpendicularly to the stretching direction. Using this procedure we obtain a set of 5-cm long, 60-μm thick, 1-mm large shavings. To reduce the influence of temperature changes and of normal stress components, we cut and glued this film on the contact in an appropriate way. We first glued a 3-mm long piece of shaving on a half of the printed circuit contact; then we glued another 3-mm piece of shaving near the first

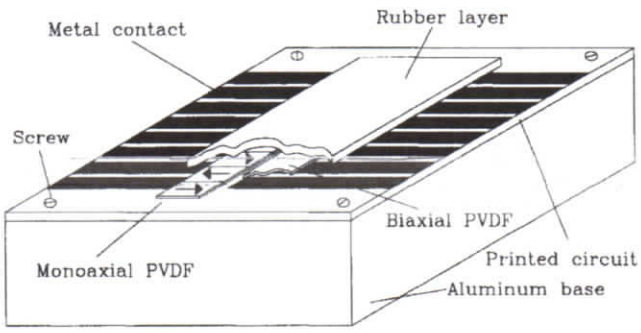

Fig. 1. A schematic of the tactile array sensor able to detect the incipiency of the slippage. Each *tactel* is composed of two transducers: one is sensitive to a combination of normal stresses while the other is sensitive to the shear stress in the arrow direction.

one. This second piece was glued upside-down and rotated of 180° on the printed circuit plane. The same procedure was followed for each contact. In such a way, only the shear stress component of the stress, in the direction of the array, is able to elicit a net charge at the electrodes. For the same reason also the pyro-electric effect is minimized.

The net charge generated by the indenter contact with the sensor is acquired using a set of 16 charge amplifiers. To avoid the saturation problem we put a resistance in parallel to the charge amplifier capacity. The time constant of the RC group was 1 s.

The outputs of the amplifiers were directly connected to a 16 channel analog-to-digital converter board, PCL812PG (Advantech Co. Ltd., Taiwan), inserted in a 80386 PC. Complete array data acquisition was performed at a sampling frequency of 100 Hz.

IV. Numerical Solution of the Direct Problem

To obtain simulated data we needed to solve the tactile direct problem in presence of friction: given the object as well as the normal and the shear force applied to it, the stress acting on the transducers inside the sensor has to be found. The following constraints must be considered.

- Friction is a very complicated phenomenon and it depends not only on the material of both the sensor and the object in contact, but also on environmental conditions, surface finishing and other uncontrollable factors. The friction coefficient is both a very simple and, at times, inadequate parameter to describe the problem.
- Even if it was possible to describe friction by Newton's law, contact between two bodies in the presence of friction is one of the most complex problems of contact mechanics, and the direct problem never admits a closed-form solution.
- A general solution for different shapes of the indenter cannot be found, even if approximations and simplifications are introduced into the problem.

Since the direct problem cannot be solved analytically, the FEM approach was used. Given the complexity of the problem, some simplifying assumptions were required to obtain the data needed to feed the tactile network. The model was made up of two parts: the pressing body and the sensor block. It

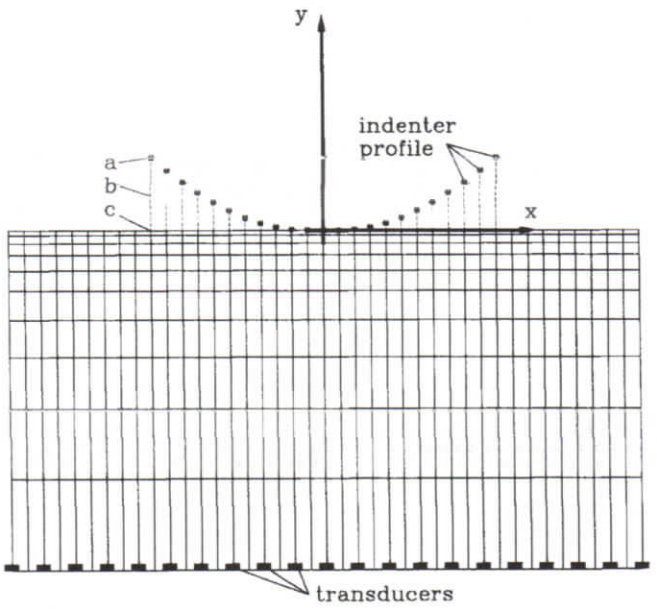

Fig. 2. Model of the sensor. The transducers are posed directly on the rigid base while the indenter is schematized by its nodes in the plane x-y connected to the sensor by means of gap elements (dashed lines). Nodes on the sides and on the surface are free, except the ones connected to the indenter and to the sensor using (b) gap elements: they are free only if the (a) indenter node and (c) the sensor node are not in contact. The gap elements $(a + b + c)$ automatically manage situations of stick and slip.

was assumed that the model extends indefinitely along the Z axis to reduce the great number of calculations of the tridimensional case. The pressing body was modeled assuming that it has infinite stiffness; hence, only the coordinates of the nodes on its profile were given. The sensor block was partitioned in a rectangular mesh representing the superficial rubber layer, where the sensor elements were ideally placed in the nodes at the sensor's base (see Fig. 2). Constraints in all three spatial directions were imposed on the base nodes to simulate the rigid base of the sensor block. The mesh of the sensor block was denser at the top surface zone, because the stress and the strain gradients are expected to be greater there. Two-dimensional, isotropic elements suitable for solid structures modeling were used to build the sensor block. Nonlinear elements were not used because the rubber in the sensor presents linear stress-strain characteristics up to 20% strain, as determined in separate stress-strain tests.

The interaction between the two bodies is simulated by using gap elements to link the nodes of the indenter with the corresponding ones of the sensor block. A gap element produces stress only when the two bodies tend to penetrate, while it lets them free to separate. The indenter was supposed to be applied only on the sensor center (see Fig. 2).

One of the most important phases at the planning stage is the mesh dimensioning. The mesh must be structured correctly; along with this, the optimal number of elements must be found for the problem to be solved. A high number of elements with a very dense mesh can lead to accurate results, but it is very penalizing in terms of computational load. On the other hand, a poorly dimensioned mesh can yield quite crude results. In this work great care was taken in dimensioning the mesh, using both time and computational load as cost parameters.

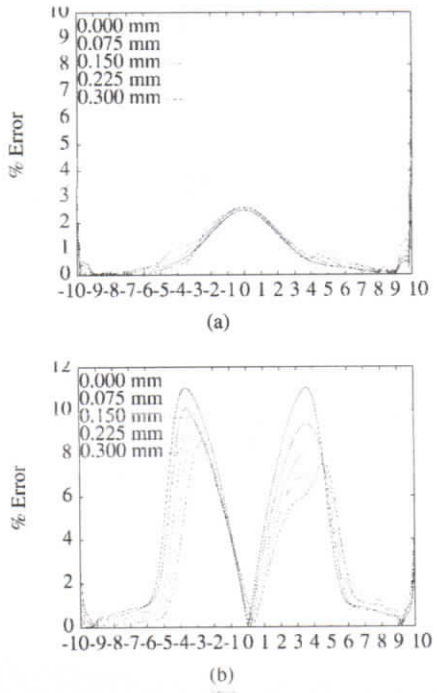

Fig. 3. (a) Percentage error curves in the determination of the normal stress component σ_y and (b) the shear stress component τ_{xy} for various tangential indentation values. On the horizontal axis the distance from the sensor center is reported.

One simulation was executed at the maximum mesh density allowed by the wave-front (bandwidth of the global stiffness matrix) limitations of the program; this large model uses 123×33 nodes to represent the sensor block. Another model was dimensioned, using practical considerations involving the number of sensors composing the array, in a 41×11 mesh.

In the following the most accurate simulation is referred to as simulation A, the other as simulation B. The simulation results samples are indicated with the subscript i (A_i and B_i), the displacement between indenter and sensor is indicated as u_x, the normal stress field value with σ_y, and the tangential stress field value with τ_{xy}.

After re-sampling the stress curve rebuilt from simulation B data using a spline third order interpolation, so as to have two arrays of the same length to compare, the following formula was used to estimate the relative error introduced by the rougher quantization:

$$\epsilon_{\sigma_y} = \frac{\left|\sigma_y^{B_i} - \sigma_y^{A_i}\right|}{\max\left|\sigma_y^{A_i}\right|} \tag{6}$$

$$\epsilon_{\tau_{xy}} = \frac{\left|\tau_{xy}^{B_i} - \tau_{xy}^{A_i}\right|}{\max\left|\tau_{xy}^{A_i}\right|}. \tag{7}$$

As can be seen from Fig. 3, where the error curves are shown in the case of a parabolic indenter with a normal penetration of 0.15 mm and five steps of tangential displacement linearly increasing from 0 mm to 0.3 mm, the error is always quite small. Table I shows that the maximum error is 11.05%, i.e., small enough to justify the use of the rougher mesh for further simulations. In addition, it is important to note that the absolute error is usually much smaller than the maximum absolute value recorded at the borders.

TABLE I
MAXIMUM PERCENTAGE ERRORS IN σ_y AND τ_{xy} FOR DIFFERENT VALUES OF TANGENTIAL DISPLACEMENT OF THE INDENTER. ON THE HORIZONTAL AXIS THE DISTANCE FROM THE SENSOR CENTER IS REPORTED

u_x	max % error in σ_y	max % error in τ_{xy}
0	3.46	11.05
0.075	4.73	10.10
0.15	6.19	9.74
0.225	7.81	9.36
0.3	9.34	8.55

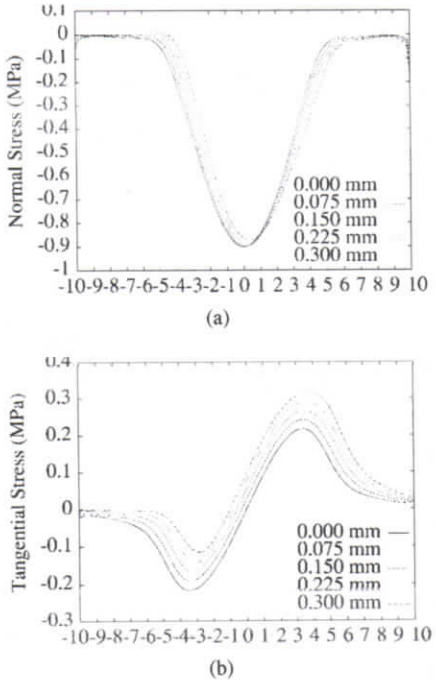

Fig. 4. (a) Normal and (b) shear stresses at the sensor array plane for various tangential indentation values. On the horizontal axis the distance from the sensor center is reported.

System geometry is shown in Fig. 2 in the case of simulation B. Fig. 4 shows the normal and shear stresses caused by a fixed normal indentation and an increasing tangential indentation, in the case of simulation A. It can be seen how τ_{xy} shapes change with the progressive increase of tangential loading while σ_y shapes show little change, while in Fig. 5 the spatial distribution of normal and shear stress fields inside the sensor block are shown for a parabolic indenter with normal and tangential load.

V. BACK PROPAGATION NEURAL NETWORKS TO DETECT INCIPIENT SLIP

Multilayer perceptrons networks trained using the backpropagation (BP) algorithm have been used in a large number of problems dealing with class discrimination and pattern recognition [14]. They have shown a particular ability in solving tactile data processing related problems [8], [9], [15], even in a noisy environment. In this work the ability of a BP network to detect incipient slippage is tested.

As we said in the introduction, we investigated about the possibility of a neural net to discriminate the incipience of the slippage using both simulated and real data. In this section we

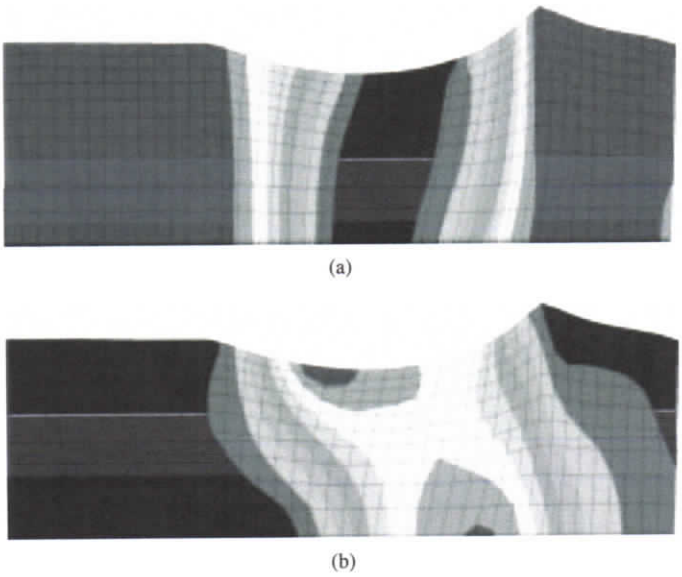

Fig. 5. This is an example of the results obtained from simulation. A section of the model of the indefinite sensor is shown while a parabolic indenter is pressed on it: the contour lines of (a) normal and (b) shear stress fields are shown in the case of both normal and tangential indentation applied to the paraboloid.

report about the preliminary dimensioning of the network and the results obtained on simulated data.

As described in Section III, it was impossible to obtain a sensor with high spatial resolution joined to an adequate sensibility: consequently our actual sensor is made of only eight tactels. Using simulation it is possible to obtain data with higher spatial resolution: as a consequence, we supposed to obtain data from a sensor having 21 sensitive sites (tactel) composed by two transducers, for a total length of 2 cm. The results of the work on this simulated data are interesting because they can elicit the behavior of the network with data that still cannot be obtained from any sensor and are also useful to select a net structure using adequate learning and recalling sets.

A. Network Design

The input data are the normal and shear stress components. Since the simulated device is composed of 21 normal stress sensitive elements and 21 shear stress sensitive elements, the input layer of the neural network is dimensioned in 42 processing elements (PE). The detection of incipient slippage is made assuming as network output the *slippage index* S_i: $S_i = \frac{Q}{\mu P}$. This implies the use of only one PE in the output layer. After dimensioning the input and the output layer of the network, the hidden layers as well as their numbers have to be dimensioned. Some neural network computational studies [16] have shown that a three-hidden-layer BP neural network is able to make any arbitrary partitioning of the input space. However, depending on the complexity of the problem, it may be unnecessary to use all the hidden layers.

Since the number of sensors in a linear array has been fixed to 42, and since it is impossible to decide in advance if all the sensors will be equally important to the sensing task, the first choice has been to dimension the input layer in 42 PE's. The output layer, as said before, has one PE.

The next design step resides in defining the hidden layers. It is necessary to recognize the progressive changes of a curve toward a certain state, with no concerns about the type of curve we are dealing with. The neural network should be able to extrapolate the elements characterizing the shape changes, and it should show a complete immunity to the curve shape itself. Two network families have been tested, starting with a one-hidden-layer structure and increasing the number of hidden layers as long as the network response was not satisfactory.

The following six networks have been designed and tested:

1) one 42 PE's hidden layer;
2) one 84 PE's hidden layer;
3) one 21 PE's hidden layer;
4) two 42 PE's hidden layers;
5) one 42 PE's and one 82 PE's hidden layers;
6) one 42 PE's and one 21 PE's hidden layers.

The activation function used in each layer strictly depends on the space to be explored and recognized. Our problem is both a classification and an approximation one: therefore, it seems appropriate to use the sigmoidal activation function

$$f(z) = \frac{1}{2}\frac{1 - e^{-z}}{1 + e^{-z}}$$

in all the layers, because this structure has shown to provide the best average response in both classification and approximation problem [17]. To minimize the maximum absolute error in the recognition of S_i the maximum error estimate has been used as error criterion. The algorithm that rules the learning phase is the *Generalized Delta Rule* in its original formulation [16]; the reason of this choice is that the standard algorithm provides the "worst case analysis," giving an estimate of the lower feature limit of the network. The square summation of the output error (SSE) has been used as error criterion.

B. Learning Parameters

The typical BP learning algorithm usually involves four parameters: *Learning Rate* (LR), *Momentum* (M), *Learning Data Noise* (LDN), and *Cycle Number* (CN) [18]. The values of LR = 0.1 and M= 0.9 [16] have been used for the first two parameters. Networks have been trained with both noise-free and noise-added (Gaussian noise with a standard deviation of 10% of the maximum stress found during the simulation) learning sets, to test the change of the performance in presence of noise. The optimal value of the CN parameter came out, from preliminary training sessions, to be 10000, even if more learning cycles were used to train the two-hidden-layers networks 4 to 6, since they have more internal states to be set properly. In none of the cases the value of 15 000 cycles was exceeded. It is worth mentioning that CN represents the maximum number of cycles that a network can reach during a training session; moreover a trigger was set in the neural net simulator program to provide a learn break mechanism when the error goes below a specified value, to prevent the network from over-learning phenomena.

TABLE II
OUTPUT ERRORS EXHIBITED BY THE NEURAL NETWORKS FOR DIFFERENT NETWORK DESIGNS IN BOTH THE LEARNING AND THE RECALLING PHASES. THE ERROR ARE ABSOLUTE ERROR REFERRED TO THE MAXIMUM SLIPPAGE INDEX VALUE OF 1

Network configuration	Learning Phase			Recalling Phase		
	Max Error	Mean Error	Std Dev	Max Error	Mean Error	Std Dev
#1	0.04922	0.00264	0.00438	0.27284	0.03558	0.03401
#2	0.05606	0.00355	0.00506	0.43712	0.04601	0.04646
#3	0.04602	0.00253	0.00416	0.26308	0.03805	0.03370
#4	0.04221	0.00250	0.00334	0.19630	0.03436	0.02856
#5	0.04311	0.00236	0.00351	0.18508	0.03416	0.02921
#6	0.04082	0.00130	0.00258	0.17709	0.03416	0.02918

C. Learning Set Design

In this work the indenter shape class has been limited to convex functions. Considering that an exhaustive learning set cannot be obtained, and a set formed by an arbitrary number of arbitrary shapes would not allow a good representation of the input class, a Taylor polynomial approach was chosen. In other words, a learning set was built using powers of x from 0 to n, and all their possible linear combinations with coefficient 1 (e.g. in the case $n = 2 : 1, x, x^2, x+x^2$). A learning set of 32 Taylor fifth order shapes (that is, all the possible combinations from $f(x) = 0$ to $f(x) = x + x^2 + x^3 + x^4 + x^5$) has been built to feed the network. A constant normal displacement of 0.15 mm and a linearly increasing tangential displacement with a step of 0.05 mm was then imposed to the indenter.

D. Design of the Recalling Sets

A properly selected recalling set would have to be fully representative of the objects the network will have to deal with in its real work place. It has to be compatible with the information embedded in the learning set, too. The recall set has been built using common shapes, giving for each of them four different examples. Indenters with the following cross sectional shapes were used:

1) flat;
2) triangular;
3) parabolic;
4) spherical;
5) exponential;
6) trapezoidal;
7) flat with parabolic edges.

E. Results With Simulated Data

The networks have been trained using an absolute maximum error trigger of 0.01, used to stop learning whenever the error becomes less than 1% with respect to the data value range ($\{-0.5, 0.5\}$), or when the cycle counter reaches the maximum cycles value (see Section V-B). The behavior of the networks in the learning phase and in the recall phase is illustrated by the values reported in Table II. The table shows that all the networks have similar behaviors.

Although a very small value of the standard deviation suggests that almost all the recall examples present an error near to the mean error, the maximum absolute error is high. The examples that caused an error over 10% have been examined, and a common characteristic was found: they were all sharp indenters near to the slipping condition. This can be justified by the fact that sharp indenters act on a few sensors, causing a bad representation of the stress curves at the network input.

It should be noted that the learning history slightly influences the performance of a network (the initial weights of the connections are generated randomly and there are oscillations during the learning phase); consequently, referring to a trained network as the "best performing" one with a narrow margin with respect to the others does not imply that *all* the other networks have a poor performance. In the preceding tests the better performance of the two-hidden-layer networks is evident, while the choice of the best performing network among #4, #5, and #6 has been slightly influenced by the learning history.

VI. A NETWORK FOR REAL DATA

When we use the real sensor we could only obtain eight couples of field sample: using this data we conducted, anyway, a preliminary experimental study.

The network input data are the normal and shear stress components. Since the experimental device is composed of eight normal stress sensitive elements and eight shear stress sensitive elements, the input layer of the neural network is dimensioned in 16 processing elements (PE). The detection of incipient slippage is made assuming as network output the *slippage index* S_i: $S_i = \frac{Q}{\mu P} = \frac{\tan(\theta)}{\tan(\theta_L)}$. This implies the use of only one PE in the output layer.

After dimensioning the input and the output layer of the network, the hidden layers as well as their number have to be dimensioned. In Section V we found that even a very simple net, with only one hidden layer with the dimension of the input layer, is able to detect the incipiency of slippage. Anyway, our data are a little bit more complex to analyze: the indenter could be in any position on the sensor. As a consequence, we chose to use the simpler double hidden layer network structure described in Section V: this structure has a first hidden layer with the same dimension of the input one (that means 16 PE) and a second hidden layer with a half of the elements (8 PE).

The other structural elements of the network, and the learning parameters, were the same than on Section V.

Working with real data we need to keep the indenter shapes class limited to a very simple and small set of convex indenter. The class is quite small because of the difficulties we encountered to obtain a high number of data. Moreover the low resolution of the sensor output implies that small

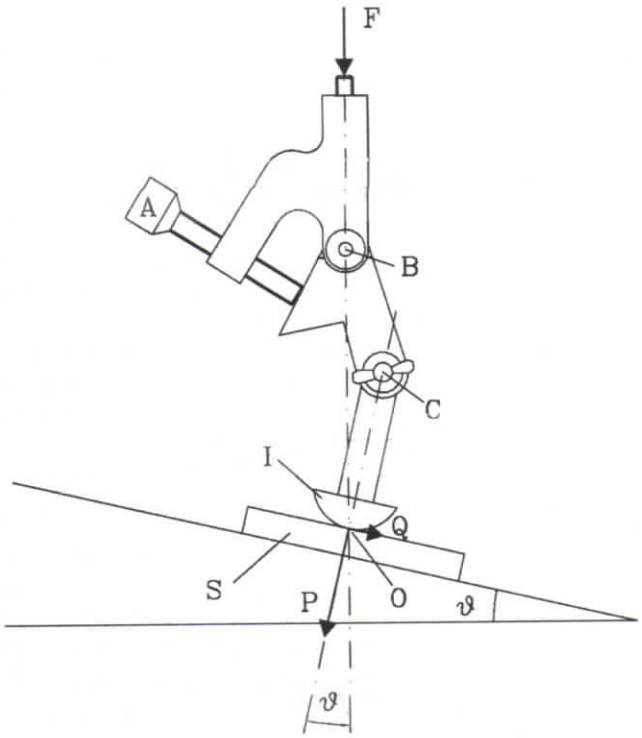

Fig. 6. A drawing of the structure used to apply the indenter on the sensor.

difference in the indenter shape does not produce noticeable output difference.

Due to the difficulties described in the experimental results section, we could only use a limited number of friction limit angles and angles of application of the indenter load.

The shape of the indenter we chose was as follows:

1) flat (4 mm wide);
2) flat (6 mm wide);
3) flat (10 mm wide);
4) cylindrical (radius 10 mm);
5) cylindrical (radius 30 mm);
6) triangular (edge angle 60°);
7) triangular (edge angle 120°);

The indenter was applied on three different positions on the sensor: centered and ± 2.5 mm from the center. As regard the friction limit angle between the indenter and the sensor we used two values (25° and 38°). We obtained the first value of critic angle distributing talcum powder on the sensor surface. We applied the force to the indenter with three angles: 0°, 15°, and 30° (the last one could only be applied when the critic angle was 38°).

Using a combination of different indenters, different friction critic angles, contact point position, and resultant angles we obtained a training set made of 25 examples and a recalling set made of 11 examples. Using the values of critical angle and angle of the resultant we obtained different values for S_i.

VII. Experimental Results

A. Experimental Setup and Preliminary Measurements

To obtain shear and normal stress field data we needed to apply a calibrated force to the sensor using different

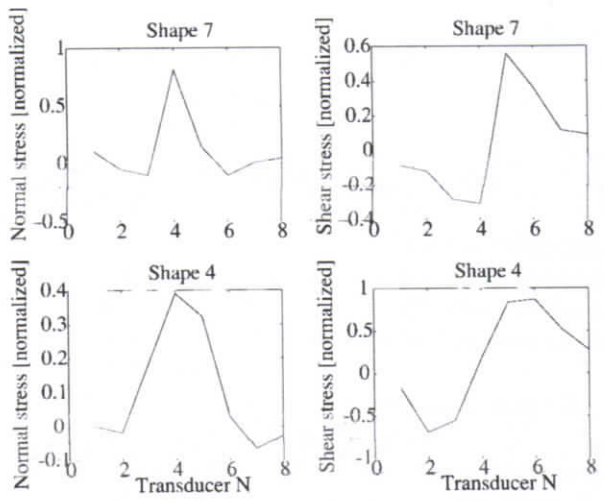

Fig. 7. Two samples of the data acquired from the sensor when pushed with two different indenter shapes: shape 4 with $\theta = 15°$, and shape 7 with no tangential load applied.

indenter. Moreover we needed to measure the critic angle between the sensor and the indenter. To have a coherent set of data, indenters was made larger than the sensor surface. It was pushed on the sensor transversely to the direction of transducers.

A simple experimental setup was built to enable us to apply a force with a given application angle and to determinate the friction critic angle (see Fig. 6). We fixed the sensor on a micrometrical table that may be tilted of a known angle. Then, we pushed the indenter on the sensor using a small hand pillar press and a suitable mechanical structure.

This structure (see Fig. 6) is made of three pieces of aluminum joined by two hinges **B** and **C**. The indenter **I** is screwed to the structure. Screw **A** and the wing nut in **C** allow to adjust the indenter position in such a way it is perpendicular to the sensor surface **S**. Moreover, the direction of the force applied by the press, passes for the contact point **O**. When we apply the load, hinge **C** is blocked while **B** may only turn in the counter clockwise direction. Force **F** is then applied without generate any torque in the contact area. The force application angle θ is easily measured.

Before stress data acquisition we measured the friction critic angle θ_L. The procedure consists in tilting the sensor (adapting the structure and the indenter in the meantime) until a rotation around hinge **B** happens because of a slippage of indenter **I**. This measure must be carried out very carefully, applying the indenter gently to avoid stick phenomenon.

B. Data Acquisition

Using the experimental setup we just described, we acquired data from the charge amplifiers for 10 s while we were pressing an indenter against the sensor. We then selected the sample with the highest normal stress value. This procedure was repeated for each element of the learning and of the recalling sets. Two examples of the acquired data, for two shapes of indenter, are shown in Fig. 7. An important thing we need to point out is that the sensor was not calibrated, as can be seen

discrimination by a tensorial tactile sensor array and neural inversion algorithms," *IEEE Trans. Syst., Man, Cybern.*, vol. 25, pp. 933–946, June 1995.
[11] K. L. Johnson, *Contact Mechanics*. Cambridge, U.K.: Cambridge Univ. Press, 1985.
[12] A. Caiti, G. Canepa, and D. De Rossi, "Tactile sensing for stable grasp," in *Engineering Systems with Intelligence*, S. G. Tzafestas, Ed. Amsterdam, The Netherlands: Kluwer, 1991, pp. 257–264.
[13] D. De Rossi, G. Canepa, F. Germagnoli, G. Magenes, A. Caiti, and T. Parisini, "Skin-like tactile sensor arrays for contact stress field extraction," *Mater. Sci. Eng.*, vol. 1, pp. 23–36, 1993.
[14] B. Widrow and M. L. Lehr, "30 years of adaptive neural networks: Perceptron, madaline and backpropagation," *Proc. IEEE*, vol. 78, pp. 1415–1442, Sept. 1990.
[15] Y. C. Pati, P. S. Krishnaprasad, and M. C. Peckerar, "An analog neural network solution to the inverse problem of 'early taction'," *IEEE Trans. Robot. Automat.*, vol. 8, no. 2, pp. 196–211, 1992.
[16] J. L. McClelland and D. E. Rumelhart, *Explorations in Parallel Distributed Processing*. Cambridge, MA: MIT Press, 1988.
[17] A. R. Barron, "Universal approximation bound for superposition of a sigmoidal function," *IEEE Trans. Inform. Theory*, vol. 39, pp. 930–945, 1993.
[18] C. C. Klimasauskas and J. P. Guiver, *NeuralWorks Networks I*, Neuralware Inc., 1988.

Gaetano Canepa was born in La Spezia, Italy, in 1965. He received the "Laurea" degree in electronic engineering from the University of Pisa, Pisa, Italy, in 1990 and the doctorate degree in robotics from the University of Genova, Genova, Italy, in 1995.

His main research interests are in the area of data analysis and hardware design of sensors. He has been carrying out research on ultrasonic, acceleration, force, and tactile sensors.

Rocco Petrigliano was born in Valsinni, Italy, in 1968. He received the "Laurea" degree in electronic engineering from the University of Pisa, Pisa, Italy, in 1996. His thesis title was "Design and realization of a tactile sensor sensible to shear and normal stress."

His main interests are in the area of the hardware design of sensors.

Matteo Campanella was born in Messina, Italy. He received the "Laurea" degree in electronic engineering from the University of Pisa, Pisa, Italy, in 1993. His thesis title was: "Incipient slippage detection using neural networks."

He is a contributor to the Italian monthly magazine *Login*. His main interests are now focused on distributed electronic networks.

Danilo De Rossi was born in Genova, Italy. He received the "Laurea" degree in chemical engineering from the University of Genova.

From 1976 to 1981, he was a Research Fellow with the Institute of Clinical Physiology, Italian National Research Council, where he is currently Leader of the Sensor Group. Since 1982, he has been with the School of Engineering, University of Pisa, Pisa, Italy, where he is currently Professor of Biomedical Engineering. He has also worked in France, the United States, Brazil, and Japan. His scientific interest is focused on the physics of organic and polymeric material for signal transduction and modeling, and on the design of sensors and actuators for bioengineering and anthropomorphic robotics.